

Optical Emission from Excess Si Defect Centers in Si Nanostructures

X. L. Wu,^{1,*} S. J. Xiong,¹ G. G. Siu,² G. S. Huang,¹ Y. F. Mei,² Z. Y. Zhang,¹ S. S. Deng,¹ and C. Tan¹

¹National Laboratory of Solid State Microstructures and Department of Physics, Nanjing University, Nanjing 210093, People's Republic of China

²Department of Physics and Materials Science, City University of Hong Kong, Kowloon, Hong Kong, People's Republic of China
(Received 21 August 2002; published 9 October 2003)

Four groups of Si nanostructures with and without β -SiC nanocrystals were fabricated for clarifying the origin of a blue emission with a double-peak structure at 417 and 436 nm. Spectral analyses and microstructural observations show that the blue emission is related to the existence of excess Si atoms in these Si nanostructures. The energy levels of electrons in Si nanocrystals with vacancy defects formed from the excess Si atoms are calculated and the characteristics of the obtained density of states coincide with the observed double-peak emission. The present work provides a possible mechanism of the blue emission in various Si nanostructures.

DOI: 10.1103/PhysRevLett.91.157402

PACS numbers: 78.55.Mb, 78.30.Fs, 78.66.Db

Since the discovery of porous Si (PS) with room-temperature visible emission [1,2], many studies have focused on fabrications and blue-emitting properties of Si nanostructures [3–10], because blue emission is of great importance for applications in modern optoelectronics. However, the complexity of microscopic details and little theoretical research activities make many blue-emitting origins still unclear or controversial. This is the case for the blue photoluminescence (PL) with a double-peak structure at 417 and 436 nm, which was frequently observed in many Si nanostructures such as anodized microcrystalline Si thin films [11], Si⁺-implanted SiO₂ films [12], strongly oxidized PS [13], and Pb(Zr_xTi_{1-x})O₃-embedded PS [14]. To improve device performance and materials quality, it is necessary to clarify the blue PL origins from experiments and theory. In this work, we first establish that Si nanostructures produced by four completely different means, laser ablation, C₆₀ precursors, electrochemical etching, and ion implantation, produce common luminescence features, especially a double-peak emission at 417 and 436 nm. We next establish that the emission is due to Si nanostructures and there is no size dependence which rules out quantum confinement effect. We next present calculations for the simplest defect common to all structures, a Si vacancy, and demonstrate that a specific concentration is required to explain the observed peaks.

Group A was obtained using laser ablation of a polycrystalline SiC target (KrF excimer pulsed irradiation of 248 nm in wavelength, 30 ns in pulsed width, and 5 Hz in frequency). The average laser energy density was 200 mJ/cm². Samples were put on a hot stage kept at about 650 °C. The substrates used in samples A1 and A2 were <100>- and <111>-oriented *p*-type Si wafers with a resistivity of 5–10 Ω cm, respectively. The deposition chamber was initially pumped down to lower than 10⁻³ Pa. The thicknesses of the deposited films were ~300 nm. Figure 1(a) shows the PL spectra of samples A1 and A2. One can see that a blue emission with double-

peak structure at 417 and 436 nm occurs. The two peaks have an energy interval of about 0.13 eV and their positions remain unchanged, but their intensities vary with sample. The Fourier-transform infrared (FTIR) spectra of the two samples are similar, as shown in the inset of Fig. 1(a). The 790 cm⁻¹ vibration band corresponds to the TO phonon absorption peak of β -SiC [15], indicating that group A contains a β -SiC component. Figures 2(a) and 2(b) show the high-resolution transmission electron

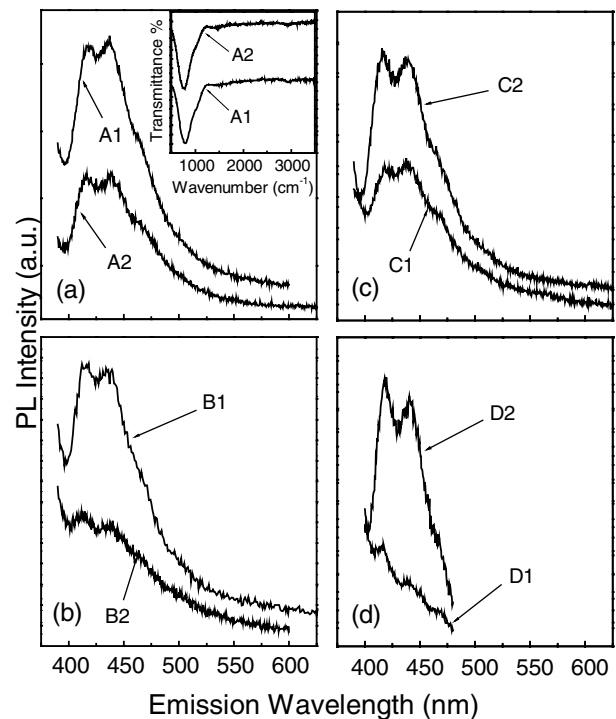


FIG. 1. (a)–(d) PL spectra of four groups of Si nanostructures A–D, taken on a Hitachi 850 fluorescence spectrophotometer under excitation with the 370 nm line of a Xe lamp. The inset of (a) shows the FTIR absorption spectra of samples A1 and A2, taken on a Nicolet 170SX spectrometer.

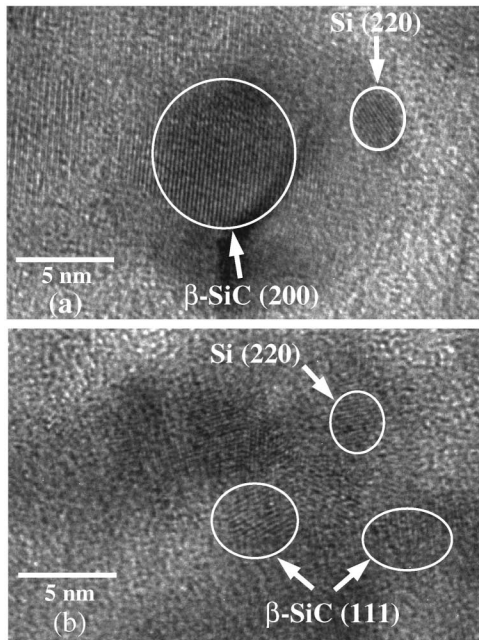


FIG. 2. HRTEM images of samples (a) A1 and (b) A2, taken on a Phillips CM 200 FEG TEM. The existence of Si and β -SiC nanocrystals can clearly be observed. The sizes of Si nanocrystals are generally about 2.6 nm.

microscopy (HRTEM) images of samples A1 and A2, respectively. It can be seen that the two samples contain both β -SiC and Si nanocrystals. The sizes of Si nanocrystals are generally 2.6 nm, but the sizes of β -SiC nanocrystals are larger in sample A1 than those in sample A2. This implies that the blue PL cannot arise from the band-to-band recombination in the quantum confined β -SiC nanocrystals. After sample A2 was annealed at 800 °C in N_2 for 30 min, our HRTEM image shows that the average β -SiC crystallite size increases from 4.4 to 5.9 nm. The fact that the peak position stays unchanged supports this conclusion.

Group B was taken by annealing the C_{60} -coupled PS samples under different temperatures in N_2 . The coupling experiments have been reported in our previous literature [16]. Figure 1(b) shows the PL spectra of two samples B1 and B2 annealed at 1100 °C in N_2 for 60 min (the two samples have the initial PL peaks from PS at 590 and 650 nm). Obviously, the blue PL spectra are similar to those of group A. In group B, the presence of Si and β -SiC nanocrystals has been verified in our previous work [17]. An investigation on the growth mechanism of β -SiC nanocrystals indicates that the formation of β -SiC nanocrystals starts at the interface between the substrate and the C_{60} cluster and continues by diffusion of Si through the already formed SiC. This implies that some Si nanocrystals arise from crystallization of excess Si atoms around β -SiC nanocrystals.

Group C was directly fabricated from electrochemical etching of n -type Si wafers with $\langle 111 \rangle$ orientation and

0.002–0.005 Ω cm resistivity. The anodization was carried out in a solution of HF: C_2H_5OH = 1:2 with a current density of 70 mA and an anodic time of 5 min. The thicknesses of the porous layers were measured to be ~ 30 μ m. Sample C1 was fabricated under illumination of a W lamp so that the Si nanocrystals have small sizes. Sample C2 was anodized in the dark for 5 min, followed by annealing at 1050 °C in N_2 for 20 min. Figure 1(c) shows the PL spectra of samples C1 and C2. A similar double-peak PL structure can be observed. The PL intensity is larger in sample C2 than that in sample C1. To rule out the possibility for the blue PL to be from the band-to-band recombination in the quantum confined Si nanocrystals, we performed the atomic force microscope (AFM) observations of samples C1 and C2 and present the corresponding results in Figs. 3(a) and 3(b). It can be seen that the sizes of Si nanocrystals are smaller in sample C1 than those in sample C2. Figure 3(c) shows the Raman spectra of samples C1 and C2 with the peak positions at 495 and 504 cm^{-1} , respectively. This result means that samples C1 and C2 have the average crystallite sizes of 1.8 and 2.6 nm [9]. Therefore, the PL peak energies have no crystallite size dependence. We further found that after the samples were stored in air for three months, the blue PL has no change in peak position and intensity. Oxygen passivation at the surface of crystallite can cause a reduction of the effective size [18,19], so the PL with a fixed peak position should not arise from the quantum confinement on Si nanocrystals. In PS, the three-region model presented by Kanemitsu *et al.* [20] has successfully been adopted to explain the red-emitting origin [21,22]. However, the present PL intensity is generally higher in the sample with large crystallite sizes than that with small crystallite sizes. Following the original idea by Kanemitsu *et al.*, we can infer that the blue PL should not originate in silicon-oxygen related surface states.

Group D was obtained by room-temperature Si^+ implantation into $\langle 111 \rangle$ -oriented n -type Si wafers with a resistivity of 5 Ω cm under an energy of 140 keV. Sample D1 was fabricated at an implantation dose of 1×10^{15} cm^{-2} . Sample D2 was initially produced at an implantation dose of 2×10^{15} cm^{-2} , followed by rapid thermal annealing at 800 °C in N_2 for 40 s. Figure 1(d) shows the PL spectra of samples D1 and D2. Clearly, a similar blue emission with double-peak structure at 417 and 436 nm can be observed. The PL intensities are far larger in sample D2 than that in sample D1. Since sample D2 has larger crystallite sizes than sample D1 [23], the surface state models are not suitable candidates for the blue PL origin. Further FTIR measurements found that samples D1 and D2 have only a very weak Si-O-Si vibration band at 1025 cm^{-1} , indicating that group D is Si excess.

For all the aforementioned Si nanostructures with the blue PL, a sharp feature is the existence of excess Si atoms

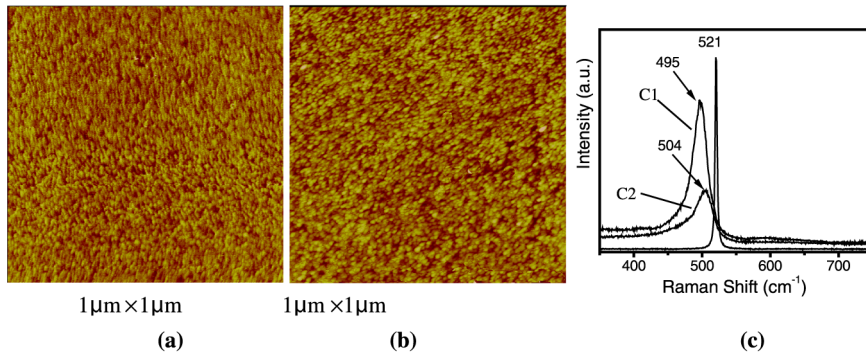


FIG. 3 (color online). AFM pictures of samples (a) C1 and (b) C2, taken on Park Scientific Instruments with Autoprobe CP. (c) Raman spectra of samples C1 and C2, taken on a T64000 triple Raman system. The Raman peak from single crystal Si at 521 cm^{-1} is also shown for comparison.

that form small Si nanocrystals. From the obtained TEM results, the mean sizes d and size distributions (standard deviation Δ) of Si nanocrystals can be characterized by a log-normal function [24] to be $d = 2.6 \text{ nm}$ for all the samples and $\Delta = 1.14, 0.74, 0.88,$ and 1.22 nm for samples A1, B1, C2, and D2, respectively. The Δ values are smaller in samples A2, B2, C1, and D1. The sizes of Si nanocrystals are in the range of 1–4 nm in all the fabricated Si nanostructures. Therefore, Si-related defect centers may be the source of the blue double-peak PL.

To further provide evidence of the nature of the defects, we calculate the density of states of electrons in a defective nanocrystal formed from excess Si atoms. Since the crystalline structure of the nanocrystal is usually incomplete, we assume that these excess Si atoms locate within a sphere and form a diamond lattice with a lot of randomly distributed vacancy defects. For such a structure we can calculate the energy levels by using the method of linear combination of atomic orbitals (LCAO). We take into account the $2s$ and $2p$ orbitals of Si atoms and the nearest neighbor hopping integrals in the calculation. We use the empirical tight-binding parameters from Ref. [25]. By this way we can establish a $4N \times 4N$ Hamiltonian matrix with N being the total number of atoms in the nanocrystal. The energy levels can be obtained by directly diagonalizing the matrix. In Figs. 4(a) and 4(b) we plot the density of states (DOS) of small Si spheres of radius 1.3 nm and with different defect densities. It can be seen that by introducing the vacancy defects in the nanocrystal several defect levels appear in the energy gap. Especially, among them there appear two small peaks near the edge of the valence band indicated by arrows, which are separated by $\delta \approx 0.15 \text{ eV}$ energy. This structure is robust to the randomness of the structure as well as the change of size and defect density. In Fig. 4(c) we plot the partial density of states (PDOS) at the sites next to the vacancies. The energy differences between the two peaks and the highest peak of the conduction band are 3 and 2.85 eV, just corresponding to the measured emission peaks at 417 and 436 nm, respectively. In such structures the wave vectors are no longer good quantum numbers, but there may exist other physical ingredients prohibiting transitions between states shown in the curves of DOS. Nevertheless, the structures of DOS and PDOS can still provide the basic information on the possible transitions of the sys-

tem. As no such peaks exist in the gap of spectrum of nanocrystals without vacancy defects [the dotted line in Fig. 4(a)], we can conclude that these emissions originate from the states produced in the gap by vacancies in Si nanocrystals formed with excess Si atoms. This is further confirmed by the calculation of the average squared optical matrix element along the x direction as shown in Fig. 5. The double peaks, corresponding to the observed

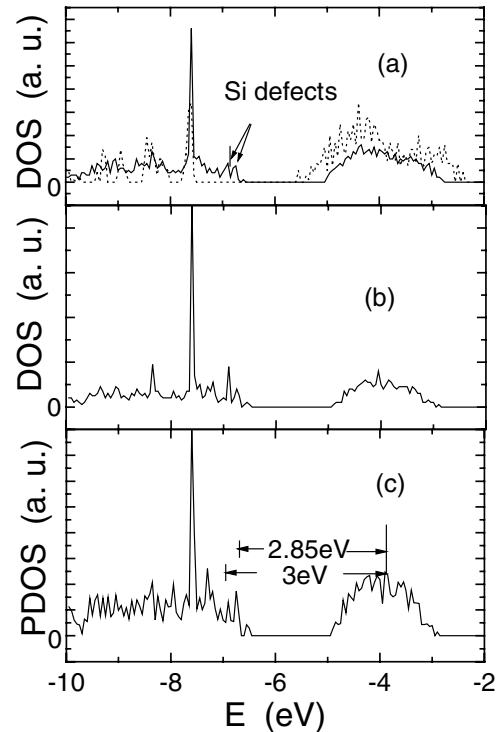


FIG. 4. (a) The calculated density of states (DOS) for Si nanocrystals of radius 1.3 nm. The calculation was carried out by using the LCAO method and tight-binding parameters of Ref. [25]: the levels of $2s$ and $2p$ states in a Si atom are $\epsilon_s = -13.5 \text{ eV}$ and $\epsilon_p = -7.58 \text{ eV}$, respectively; the nearest neighbor hopping integrals are $V_{ss\sigma} = -2.08 \text{ eV}$, $V_{sp\sigma} = 2.48 \text{ eV}$, $V_{pp\sigma} = 2.72 \text{ eV}$, and $V_{pp\pi} = -0.72 \text{ eV}$. The solid line is for the Si sphere with vacancy defects of density $p = 0.3$, while the dotted line is for the Si ball without vacancies. (b) DOS for the Si sphere with defect density $p = 0.4$. Other parameters are the same as those in (a). (c) The partial density of states at sites next to vacancies. The parameters are the same as those in (b).

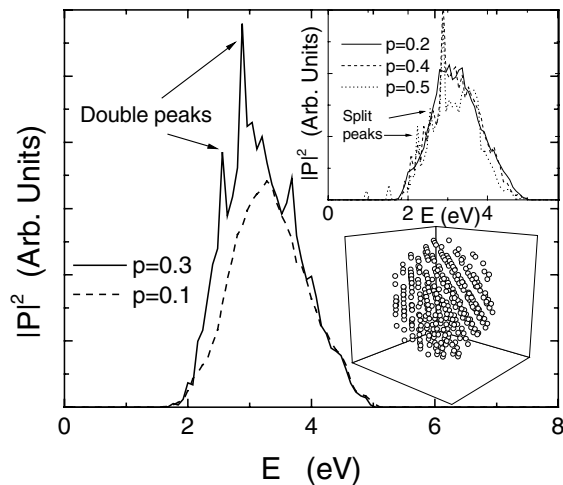


FIG. 5. Average squared optical matrix element as a function of the transmission energy for the cases of $p = 0.3$ and 0.1 . Other parameters are the same as those in Fig. 4. In the upper inset the curves for $p = 0.2, 0.4,$ and 0.5 are shown for comparison. The lower inset sketchily shows atom positions in a defective nanocrystal with $p = 0.3$.

PL spectrum, are obviously seen in the case with enough vacancies ($p = 0.3$), and are absent for smaller vacancy densities ($p = 0.1$ and 0.2). For larger vacancy densities ($p = 0.4, 0.5$), these peaks exist but are split. Because of the existence of vacancies the sphere shape for the nanocrystal used in the calculation has no crucial effect on the results. As can be seen from the structure shown in the lower inset of Fig. 5, the sphere surface has been distorted owing to the existence of vacancies in the case of $p = 0.3$.

In conclusion, we have fabricated four groups of Si nanostructures with and without β -SiC nanocrystals for clarifying the origin of the blue double-peak PL at 416 and 437 nm, which was often observed in a number of Si nanostructures. Spectral analyses and microstructural observations reveal that the blue PL is related to the existence of excess Si atoms formed during sample fabrication. A theoretical calculation on electronic states of nanocrystals formed with excess Si atoms further reveals that reaching a specific density of Si vacancies in nanocrystals is necessary for the observed double-peak emission.

This work was supported by Grants (No. 60076007, No. 10074029, No. 60276005, and No. 10225416) from the Natural Science Foundations of China. Partial support was from the Trans-Century Training Programme Foundation and the EYTP for the Talents by the State Education Commission and the special funds for Major State Basic Research Project No. G001CB3095 of China.

*Corresponding author.

Email address: hkxlwu@nju.edu.cn

- [1] For a review, see A. G. Cullis, L. T. Canham, and P. D. J. Calcott, *J. Appl. Phys.* **82**, 909 (1997).
- [2] J. L. Gole, F. P. Dudel, and D. Grantier, *Phys. Rev. B* **56**, 2137 (1997).
- [3] L. Tsybeskov, Ju. V. Vandyshev, and P. M. Fauchet, *Phys. Rev. B* **49**, 7821 (1994).
- [4] H. Tamura, M. Ruckschloss, T. Wirschem, and S. Vepřek, *Appl. Phys. Lett.* **65**, 1537 (1994).
- [5] A. J. Kontkiewicz, A. M. Kontkiewicz, J. Siejka, S. Sen, G. Nowak, A. M. Hoff, P. Sakthivel, K. Ahmed, P. Mukherjee, S. Witanachchi, and J. Lagowski, *Appl. Phys. Lett.* **65**, 1436 (1994).
- [6] T. Matsumoto, J. Takahashi, T. Tamaki, T. Futagi, and Y. Kenemitsu, *Appl. Phys. Lett.* **64**, 226 (1994).
- [7] P. Mutti, G. Ghislotti, S. Bertoni, L. Bonoldi, G. F. Cerofolini, L. Meda, E. Grilli, and M. Guzzi, *Appl. Phys. Lett.* **66**, 851 (1995).
- [8] Q. Zhang, S. C. Bayliss, and D. A. Hutt, *Appl. Phys. Lett.* **66**, 1997 (1995).
- [9] X. L. Wu, F. Yan, X. M. Bao, N. S. Li, and L. S. Liao, *Appl. Phys. Lett.* **68**, 2091 (1996).
- [10] M. V. Wolkin, J. Jorne, P. M. Fauchet, G. Allan, and C. Delerue, *Phys. Rev. Lett.* **82**, 197 (1999).
- [11] X. Zhao, O. Schoenfeld, Y. Aoyagi, and T. Sugano, *Appl. Phys. Lett.* **65**, 1290 (1994); X. Zhao, O. Schoenfeld, J. Kusano, Y. Aoyagi, and T. Sugano, *Jpn. J. Appl. Phys.* **33**, L649 (1994).
- [12] W. Skorupa, R. A. Yankov, E. Tyschenko, H. Fröb, T. Böhme, and K. Leo, *Appl. Phys. Lett.* **68**, 2410 (1996); W. Skorupa, R. A. Yankov, L. Rebohle, H. Fröb, T. Böhme, K. Leo, I. E. Tyschenko, and G. A. Kachurin, *Nucl. Instrum. Methods Phys. Res., Sect. B* **120**, 106 (1996).
- [13] V. V. Filippov, P. P. Pershukovich, V. V. Kuznetsova, V. S. Khomenko, and L. N. Dolgii, *J. Appl. Spectrosc.* **67**, 852 (2000).
- [14] Q. W. Chen, D. L. Zhu, C. Zhu, J. Wang, and Y. G. Zhang, *Appl. Phys. Lett.* **82**, 1018 (2003).
- [15] L. S. Liao, X. M. Bao, Z. Yang, and N. B. Min, *Appl. Phys. Lett.* **66**, 2382 (1995).
- [16] X. L. Wu, S. J. Xiong, D. L. Fan, Y. Gu, X. M. Bao, G. G. Siu, and M. J. Stokes, *Phys. Rev. B* **62**, R7759 (2000).
- [17] X. L. Wu, G. G. Siu, M. J. Stokes, D. L. Fan, Y. Gu, and X. M. Bao, *Appl. Phys. Lett.* **77**, 1292 (2000).
- [18] J. C. Vial, A. Bsiesy, F. Gaspard, R. Herino, M. Ligeon, F. Muller, R. Romestain, and R. M. Macfarlane, *Phys. Rev. B* **45**, 14 171 (1992).
- [19] G. Fishman, I. Mihalcescu, and R. Romestain, *Phys. Rev. B* **48**, 1464 (1993).
- [20] Y. Kanemitsu, H. Uto, and Y. Masumoto, *Phys. Rev. B* **48**, 2827 (1993); **48**, 2238 (1994).
- [21] Y. Kanemitsu, T. Ogawa, K. Shirashi, and K. Takeda, *Phys. Rev. B* **48**, 4883 (1993); Y. Kanemitsu, *Phys. Rev. B* **48**, 12 357 (1993).
- [22] X. L. Wu, G. G. Siu, S. Tong, Y. Gu, X. N. Liu, X. M. Bao, S. S. Jiang, and D. Feng, *Phys. Rev. B* **57**, 9945 (1998).
- [23] X. L. Wu, T. Gao, X. M. Bao, F. Yan, S. S. Jiang, and D. Feng, *J. Appl. Phys.* **82**, 2704 (1997).
- [24] K. Tsunetomo, A. Kawabuchi, H. Kitayama, Y. Osaka, and H. Nasu, *Jpn. J. Appl. Phys.* **29**, 2481 (1990).
- [25] P. Vogl, H. P. Hjalmarson, and D. J. Dow, *J. Phys. Chem. Solids* **44**, 365 (1983).